# LEVEL II

12

B.S.

INTERIM (MIDTERM) TECHNICAL REPORT

(78 June 01)

ARPA Order No. 2840, Amend. 10

Program Code No. 7E20

Contractor: University of Colorado
Boulder, Colorado 80309

Contract Date: 78 December 01

421

Contract Amount: $40,910

Contract No.: (15) N00014-77-C-0115; ARPA Order-2840

Contract Expiration Date: 78 November 30

Title: (6) Optical and Discharge Studies of Novel Electronic Transition Laser Species.

Principal Investigator: (10) Stephen R. Leone
(303)492-5128

(12) 33 pp



(9) Interim rept.,

(11) 1 Jun 78





78 [illegible] 05 013

78 08 03 12

088 400

Technical Report Summary

A program has been developed to use spectroscopic insight and laboratory experiments to identify potentially important new laser candidates.

An innovative series of visible and ultraviolet lasers on high temperature diatomic molecules has been discovered. To date both $S_2$ and $Te_2$ have been demonstrated to lase by optical pumping. Because of unique features of the diatomic molecular states, these molecules have potential to make highly efficient laser devices for DoD applications.

In particular, $S_2$ has numerous strong lasing transitions in the blue-green region of the spectrum for ONR applications, and many other laser lines in both the ultraviolet and red. The $S_2$ laser lases to high vibrational levels in the ground state. These levels are not populated at the 600°C necessary to form the dimers. Thus direct excitation schemes could produce very efficient conversion of energy to laser output.

The $S_2$ laser is able to withstand high power densities without degradation. It has all the usual desirable properties of gaseous systems for high average power and repetition rate. In addition the output will be line tunable over broad wavelength ranges. Collisions with rare gases serve to redistribute excited levels, but not quench the $S_2^*$.

Many other laser-suitable molecular species have been identified as well, by noting the desirable spectroscopic features of the $S_2$ molecule. $Te_2$ has already been shown to lase with the same efficiency as $S_2$. Other candidates just within group VI elements include SO, $Se_2$, TeS, TeO, TeSe, and SeS.

Considerable effort has been expended on the design and construction of a high temperature, fast current pulse discharge laser. The characteristics

next page

of electric discharges in sulfur ($S_2$) vapor are very good. We observe uniform, bright glow discharges up to pressure path lengths of 300 torr-cm in pure sulfur vapor, and to higher pressures with added helium. The lasing capability of $S_2$ by direct electric discharge excitation is currently being tested.

A series of wavelength tunable photolysis experiments have been carried out on the gas phase molecule $HgI_2$. In these experiments the quantum yield of excited $I(^2P_{1/2})$ atoms is determined to be unity at the peak of the first long wavelength absorption band. $HgI_2$ might make an interesting new source of $I^*$ for the 1.315 μm $I^*$ laser, since the photolysis products rapidly recombine in a completely reversible way to produce the parent molecule. A preprint of this work is enclosed with this report.



Technical Report

Optical pumping studies of the molecular $S_2$ ($B^3\Sigma_u^- - X^3\Sigma_g^-$) laser have been extended to include pumping of levels from V' = 0 to V' - 7 using the tunable dye laser. Lasing transitions from each of these vibrational levels in the excited B state have been mapped. The excimer laser acquired under this contract (Tachisto) was used to successfully pump the B-X transition in $S_2$ also. The 308 nm line of the XeCℓ excimer laser overlaps with one line of the (2,0) band of $S_2$ (B-X), providing an efficient pump source for the molecular $S_2$ laser. A series of strong laser transitions from $S_2$ occur in the 480-500 nm region, and are listed below.

| line (nm) | tentative lasing band |
|---|---|
| ~474 | ( 2,17 ) |
| ~486 | ( 2,18 ) |
| ~501 | ( 2,19 ) |
| ~517 | ( 2,20 ) |

The first phase of development of the meter long high temperature laser discharge cell involved extensive materials testing to determine suitable seal configurations and construction materials. It was found that sulphur vapor at 600°C and high pressures (1 Atm.) is extremely corrosive towards nearly all metals. Deterioration of the metal electrode surfaces from this effect cannot be tolerated in a sealed-off laser system. Two metals which resist the attack of the hot sulfur vapor are gold and tantalum. Gold is extremely inert at all temperatures; tantalum is only slightly reactive with sulfur at temperatures above 600°C. Because of the ease of machining tantalum, its good electrical conductivity, and its much lower cost it was selected for the electrode material.

Continued testing of a ceramic tube design for the high temperature transverse discharge laser device revealed difficulties which require further refinement of assembly technique before a reliable construction can be achieved. Prior to any assembly steps, extensive testing of the seal configuration was carried out. The original plan, that of using Inconel "C" rings as the vacuum seal for the electrical feedthroughs, was tested at room temperature. Using a variety of precious metal

platings and several stud flange designs, numerous failures of the vacuum were encountered. Microscopic examination of the components indicated that the "c" rings are apparently frequently imperfect, preventing a good seal to be made.

A second design using a conflat type flange on the stud and a 2 mil gold washer crushed against a 9 micron polished flat on the ceramic tube held tight vacuum at room temperature. During heating, however, a crack in one seal developed at the feedthrough hole in the ceramic tube. This seal failed at a very low ~200°C. Further heating of the test cell resulted in propagation of the crack around the tube, similar to cracks in pyrex. This behavior was completely unexpected. Microscopic examination of the assembly showed that this stud had been slightly off center when tightened and the crack was probably caused by this unequal stress. It is apparent from these difficulties that a highly reliable device cannot be made using such seal configurations, without further refinement.

At this time it appears that the ceramic tube design could be made to work with some small modifications. If successful, the laser cell will be far more rugged and will withstand higher temperatures than ordinary quartz-to-metal seals. However, in order to make more rapid progress on actually testing the lasing capability of the sulfur system, an alternate design approach has been employed. This approach, using a quartz envelope, is quite straightforward and the cell has been constructed and holds vacuum to appropriate temperatures. We feel, however, that further effort on the ceramic tube design is warranted for future high temperature laser species work.

The new high temperature cell design was developed using quartz as the construction medium. The general layout of the design was left unchanged, alterations being made primarily to the sealing configuration.

Quartz sidearms were sealed onto a 44 mm OD quartz tube every 10 cm. To these sidearms were attached a graded seal and pyrex to tungsten seals, holding the tantalum segmented electrodes. The length of the sidearm was 2", which extended to the edge of the firebrick oven. Assembly of the tube was straightforward. The electrodes were held in place inside the tube with a fixture and the sidearm sealed on.

The ends of the main laser tube were sealed lengths of 16 mm OD tubing to which Brewster windows had been attached with high temperature quartz transfer tape. A second tube, also equipped with a Brewster window, was sealed onto the first window at each end. These extension tubes were evacuated and sealed off. Their purpose is to extend the transition region outside of the oven to prevent thermal gradients from interferring with the optical cavity of the laser.

The electrical feedthrough seals are maintained at a lower temperature than the main body of the cell. Temperature measurements along the sidearm in a test cell made to these specifications indicated that the temperature gradient is ideal. 600°C temperature can be maintained in the center of the cell, while the seals remain at 300°C.

Tests made so far indicate that the quartz design is technologically adequate for laboratory testing. Nitrogen has been used as a lasing medium and has lased in the typical fashion at 337.1 nm. Current risetimes of 15 nsec are achieved in the present transverse discharge cell. A variety of tests have been made with sulfur in electrical discharges and these results are very encouraging for the $S_2$ system. The first discharge tests were made in a 1.5 meter longitudinal discharge cell, heated to 600°C to provide the sulfur dimer. With current risetimes of 500 nsec, the discharges in pure sulfur are completely uniform at pressures up to 2 torr

of the dimer. Addition of helium helps to sustain the uniform glow discharge up to sulfur dimer pressures of 6 torr. Much higher pressures will be feasible in the transverse discharge. The emission from the sulfur discharges is extremely bright. No spectral studies of this emission have been carried out as yet.

Work is now proceeding to attempt the direct electric discharge lasing capability of the $S_2$ (B-X) system.

A new study on the kinetics and photodissociation of $HgI_2$ to yield excited $I(^2P_{1/2})$ atoms has been completed. Our results indicate a unity quantum yield of production of $I^*$ at the peak of the first long wavelength absorption band. Because of the reversible nature of the photodissociation, $HgI_2$ may make an attractive source of $I^*$ for the 1.315 μm laser. This would be particularly important if the $HgI_2$ could be pumped by electrons to produce the $I^*$. A detailed preprint of these results, which is accepted for publication in J. Chem. Phys. is included with this report.

To appear in J. Chem. Phys.

# Tunable laser photodissociation of $HgI_2$: Quantum yield for formation of excited $I(5^2P_{1/2})$ atoms

Hubert Hofmann and Stephen R. Leone*

Joint Institute for Laboratory Astrophysics
National Bureau of Standards and University of Colorado
and Department of Chemistry, University of Colorado
Boulder, Colorado 80309

(Received 15 June 1978)

Abstract

Tunable-laser, infrared fluorescence techniques are used to study the detailed photodissociation dynamics of the linear triatomic molecule $HgI_2$. The quantum yield of excited $I(5^2P_{1/2})$ atoms has been measured in the first long wavelength absorption band of $HgI_2$ from 265 to 320 nm. From quantitative measurements of the yield of excited I atoms it is shown that the total absorption cross section in this region is actually composed of two distinct components. These components correspond to states leading to both excited and ground state I atoms according to the processes, $HgI_2 \xrightarrow{h\nu} HgI + I$ or $I^*$. From the time decay of the excited $I^*$ atoms as a function of $HgI_2$ pressure, the collisional deactivation rate of $I^*$ by the parent $HgI_2$ molecule has been obtained. This quenching rate constant is $4.5 \pm 0.2 \times 10^{-10}$ cm$^3$ molecule$^{-1}$ sec$^{-1}$ at T = 453 K, which is essentially a gas kinetic rate.

## INTRODUCTION

Detailed studies of photodissociation dynamics are of current interest and importance for new laser sources and numerous photochemical processes. Atomic, molecular or radical photofragments may now be generated by tunable laser light dissociation and are subsequently analyzed by a variety of techniques to determine the detailed quantum states in which the fragments are produced. These and similar experiments have revealed a wealth of new information regarding the electronic states of the parent molecule as well as the fundamental dynamics of the photofragmentation.[1] Some of the most extensive studies on photodissociation have been the investigations of the halogens and interhalogens using photofragment spectroscopy in molecular beams and with tunable lasers.[2-4] Based on these and other experimental and theoretical results, the photodissociation of halogens and interhalogen molecules is now relatively well understood.[5]

Since the early prediction of photodissociation lasers[6] and the subsequent discovery of the first photodissociation laser by Kasper and Pimentel in 1965,[7] based on the sequence $CF_3I \xrightarrow{\text{uv Pump}} CF_3 + I(5^2P_{1/2})$, $I(5^2P_{1/2}) \xrightarrow{\text{Laser}} I(5^2P_{3/2}) + h\nu(\lambda = 1.315\ \mu m)$, much attention has been given to other alkyl iodides as a source of excited iodine atoms.[8-11] Many molecules in this group are efficient sources for excited $I(5^2P_{1/2})$ atoms upon photodissociation with uv light. Branching ratios and fractional yields for formation of excited and ground state iodine atoms following broad band photolysis have been obtained for a large number of these alkyl compounds and their fluorinated analogs.[10,11] Recently, lasing on the atomic iodine transition $I(5^2P_{1/2}) \rightarrow I(5^2P_{3/2})$ has also been demonstrated upon photodissociation of molecular iodine using a

dye laser as a pump in the range 5010 to 4930 Å.[12]

The continued interest in new sources for atomic iodine lasers led us to study the $I^*$ production upon photodissociation of $HgI_2$ over a broad wavelength range. In this paper we investigate several aspects of photodissociation in the linear triatomic molecule $HgI_2$, for which very little is known concerning the nature of the different absorption bands. Specifically we wished to determine whether any of the absorption bands dissociate to excited $I^*$ atoms. Such metal-halogen molecules could make attractive sources for photodissociative $I^*$ lasers because of their ability to recombine and preserve the identity of the parent compound. In addition, stimulated emission from $HgBr(B^2\Sigma)$ and $HgI(B^2\Sigma)$ states has been observed after photodissociation of the triatomic metal halides $HgBr_2$ and $HgI_2$ at a pump wavelength of 193 nm.[13,14] Since the rates of collisional deactivation by the parent molecule determine to some extent the feasibility of laser action in such photodissociation lasers, we have also measured the rate constant for the deactivation of $I^*$ in the process $I^* + HgI_2 \rightarrow I + HgI_2$. The experimental results obtained provide additional detailed spectroscopic information about the $HgI_2$ molecule,[15-18] confirming that the first long wavelength absorption continuum is due to a dissociation process of $HgI_2$ leading to the ground state $HgI(X^2\Sigma)$ molecule and both excited, $I^*(^2P_{1/2})$, and ground state, $I(^2P_{3/2})$ atoms, depending on the wavelength used in the photolysis. The experimental techniques described in the present work provide an excellent method to make quantitative measurements and identifications of photodissociation products which can be detected via infrared emission. Kinetic information for the excited products is obtained simultaneously and directly from the time development after the pulsed laser excitation.

## EXPERIMENTAL

A schematic of the experimental arrangement is shown in Fig. 1. A pulsed, frequency-doubled dye laser capable of producing an energy of 1 mJ in a 2 μsec long pulse is used as a source of photolysis. With the laser dyes Coumarin 504, Rhodamine 575, Rhodamine 6G + Ammonyx, and Rhodamine 6G, the laser is tunable over the wavelength range from 265 to 320 nm. The light passes through a uv transmitting, visible blocking filter and is subsequently directed into the heated fluorescence cell. The vapor pressure of mercuric iodide in the cell is controlled by a separately heated sidearm. Typical temperatures are, for the sidearm, 361 K, and for the cell, 453 K, measured with calibrated mercury thermometers to ±0.1 K. The temperatures are measured at the coldest points of both the cell and the sidearm. Regulated dc power supplies are used for the heaters to minimize drifts and fluctuations in temperature. A temperature stability of ±0.2 K was maintained during the measurements, which corresponds to a change in the $HgI_2$ vapor pressure of approximately ±2%.[19] The energy of the laser beam transmitted through the $HgI_2$ cell is monitored by a calibrated thermopile. The output is read by a millivoltmeter and continuously recorded on an X-T recorder. The excited iodine atoms produced upon photodissociation of $HgI_2$ are detected via their infrared emission according to the transition, $I(5^2P_{1/2}) \xrightarrow{\lambda=1.315\ \mu m} I(5^2P_{3/2})$, using a liquid nitrogen cooled InSb infrared detector viewing through a narrow band transmission filter which passes 1.3 μm. For better collection efficiency of the signal radiation a sodium chloride lens is mounted above the viewport of the oven. The signals are amplified and recorded in a transient digitizer, which is triggered by a pulse from a photodiode sampling a small portion

of the laser light. The signals are stored in a signal averager and subsequently plotted with an x-y recorder. Reproducibility of the time and amplitude of the I* fluorescence signals after signal averaging 3200 laser pulses is better than 5%. The wavelength of the laser light is measured to within ±1 Å by reflecting the laser beam with a movable mirror into a calibrated monochromator. The output of a photomultiplier tube mounted at the exit slit of the monochromator is displayed on the screen of an oscilloscope.

The mercuric iodide used in the present experiments is reagent grade and contains as its only impurities 0.02% Hg and a negligible amount of other heavy metals and metal salts according to the manufacturer's specifications. A sample of solid $HgI_2$ is inserted into the quartz fluorescence cell, which is then connected to the vacuum system, evacuated to $1 \cdot 10^{-6}$ Torr ($1.33 \cdot 10^{-4}$ Pa) rest gas pressure and subsequently sealed off.

## PROCEDURE AND RESULTS

Upon examination of the literature on the $HgI_2$ spectroscopy, it was uncertain which absorption bands might lead to the excited I* photoproduct. Our first investigation in the long wavelength absorption band at 300 nm showed immediately strong signals from an I* photoproduct. A second, more puzzling, fluorescence along the path of the laser beam was observed by eye in the violet region of the spectrum. The first bound excited state of $HgI_2$ is thought to be approximately 6 eV above the ground state.[16] Thus if the observed violet fluorescence comes from emission in $HgI_2$, it would have to come from at least a two-photon absorption. A brief experimental investigation of the spectral composition of the fluorescence using a monochromator and a photomultiplier tube detector suggests that the fluorescence arises from transitions of $HgI(B^2\Sigma \rightarrow X^2\Sigma)$. The observed fluorescence covers the wavelength range from 380 to 440 nm, similar to the fluorescence reported by Wieland[16] and identified as the HgI(B-X) transition. In our case the excitation of the $HgI(B^2\Sigma)$ state is not due to direct one-photon dissociation of $HgI_2$, since direct excitation of $HgI_2$ leading to excited $HgI(B^2\Sigma)$ state and iodine atoms upon photodissociation with a single photon at 300 nm is energetically impossible.[18] However a two-photon dissociation process leading to the $HgI(B^2\Sigma)$ state may be possible. Two other mechanisms for excitation of this state may occur: (a) $[HgI(X^2\Sigma)]_{eq} \xrightarrow{h\nu_L} HgI(B^2\Sigma)$ where $[HgI(X^2\Sigma)]_{eq}$ is the equilibrium amount of HgI present in the cell at the temperatures used, and (b) $HgI_2 \xrightarrow{h\nu_L} HgI(X^2\Sigma)$ + I or I* followed by $HgI(X^2\Sigma) \xrightarrow{h\nu_L} HgI(B^2\Sigma)$. The equilibrium amount of HgI molecules in the cell is approximately 0.1%. By adding free Hg to the cell to make the equilibrium vapor pressure of HgI greater, we observe the violet fluorescence to increase. Thus direct excitation of the HgI(B-X) transition

with the laser appears to be occurring. In addition, we calculate that as much as 5% of $HgI_2$ molecules in the beam volume may be photodissociated, producing significant densities of HgI. Several of the processes described may contribute to the observed violet fluorescence. Two of the excitation schemes require that two photons are absorbed either directly or sequentially to produce the fluorescence from the $HgI(B^2\Sigma)$ state. This is confirmed qualitatively by varying the laser power and by inserting a lens in the laser path to change the radiation density and noting that the violet fluorescence varies approximately as the square of the laser power. It is most probable that these two photon excitation mechanisms are not important when a low power light source like a deuterium lamp is used instead of a laser, as in the absorption studies of Maya.[18] In those experiments violet fluorescence was only observed after excitation with light around 205 nm which produces the excited $HgI(B^2\Sigma)$ state upon direct single photon photodissociation of $HgI_2$.

The $I^*$ signal appears not to be affected by these complex fluorescence processes. The $I^*$ signal was observed to reach its peak amplitude with the laser pulse and to decay thereafter, and it varies linearly with both laser energy and $HgI_2$ pressure, confirming that it arises from a direct dissociation process. The signals were of sufficient magnitude (signal-to-noise) and reproducibility in this wavelength region to carry out measurements both on the quantum yield as a function of wavelength and on the deactivation rate of $I^*$ with $HgI_2$.

In order to measure precisely the rate constant for collisional deactivation of $I^*$ atoms by the parent molecule $HgI_2$, numerous $I^*$ decay curves were measured as the sidearm temperature of the fluorescence cell was varied from 353 K to 381 K in steps of 2 K. This corresponds to a

total variation of $HgI_2$ vapor pressure from 7.5 mTorr to 59 mTorr.[19] The temperature of the main fluorescence cell was kept constant at 453 K. The number density of $HgI_2$ molecules, $n_c$, in the cell at each sidearm temperature is determined using the relationship, $p_s = p_c = n_c \cdot R \cdot T_c$, where $p_c$ and $p_s$ are the cell and sidearm pressures respectively, $T_c$ is the cell temperature and R the ideal gas constant. All of the observed $I^*$ quenching decays are single exponentials as expected. Figure 2 shows the inverse of the observed single exponential time decay constant, $1/\tau_{obs}$, versus the number density of $HgI_2$ molecules in the cell.

A thorough discussion of other species which are present in $HgI_2$ vapor at the temperatures used has been given by Maya.[18] From there we know that the fraction of HgI molecules being formed due to thermal dissociation is less than 0.1%. The amount of polymeric species, such as $(HgI)_n$ is also negligibly small. The number of polymers of the form $(HgI_2)_n$ is expected to be small too, since an estimated bond energy for the n = 2 species is only 1.9 kcal/mole.[18] The equilibrium constant for $Hg + I_2 \rightleftarrows HgI_2$ is $K_{eq} = 1.4 \times 10^8$ at 500 K.[20] Thus the density of iodine molecules present in the sample can be neglected as well. The fractional amount of free mercury atoms in $HgI_2$ is 0.2% as mentioned earlier. From the measured laser energy and the laser beam size, and the known absorption cross section of $HgI_2$ and its pressure, we calculate that less than 5% of the $HgI_2$ molecules within the beam volume are photodissociated by the laser pulse. Since the observed quenching is extremely rapid, and since all other possible species are present in minor amounts, we conclude that the deactivation of the $I^*$ atoms is due predominantly to collisions with the $HgI_2$ parent molecules. The long 130 msec radiative lifetime[21] of $I(5^2P_{1/2})$ atoms does not contribute to the observed decay. From diffusion

calculations and from the linear relationship between the number density of $HgI_2$ molecules and $1/\tau_{obs}$, we note that diffusion to the walls is unimportant on the actual timescales of the experiment. The rate constant for collisional deactivation of $I^*$ atoms by $HgI_2$ from the series of measurements in Fig. 2 is $k = 4.5 \pm 0.2 \times 10^{-10}$ cm$^3$ molecule$^{-1}$ sec$^{-1}$. This rate is effectively the gas kinetic collision rate of $I^*$ with $HgI_2$ at 453 K.

After completing the deactivation studies, a second experiment was carried out to measure the $I^*$ atom production upon photodissociation of $HgI_2$ as a function of the wavelength of laser light used for photolysis. The data were taken at a constant cell temperature of $T_c$ = 453 K and a constant sidearm temperature of $T_s$ = 361 K. The low sidearm temperature was selected to insure that only a small fraction of the laser light is absorbed in the cell over the entire wavelength region and so the relatively slow deactivation decay of 10 μsec could be readily extrapolated to obtain an accurate maximum amplitude at time equal to zero. Special care had to be taken so that the excitation and detection geometry did not change during these measurements as the wavelength was tuned from 265 to 320 nm. The absorption within the cell can be calculated from $I = I_0 e^{-n_c \cdot \sigma(\lambda) \cdot \ell}$, where I and $I_0$ are the transmitted and initial light intensities respectively, $n_c$ is the number density of $HgI_2$ molecules in the cell ($2.6 \times 10^{14}$ cm$^{-3}$ at the temperatures used), $\ell$ is the pathlength of the fluorescence cell (9 cm), and $\sigma(\lambda)$ the absorption cross section ($1.5 \times 10^{-17}$ cm$^2$ at $\lambda$ = 270 nm).[18] Using these values we calculate a maximum absorption of the laser at $\lambda$ = 270 nm of less than 4%, and less than 1% at 320 nm.

An independent measurement of the absorption cross section of $HgI_2$

for a cell temperature of $T_c$ = 453 K was made using a 5 cm pathlength cell and a sidearm temperature of $T_s$ = 405 K, which corresponds to a vapor pressure of 0.28 Torr. The spectrum of $HgI_2$ as well as a spectrum of the empty absorption cell were recorded with a commercial spectrometer. The spectral resolution was 1 nm. The sidearm temperature was stable to ±0.2 K, which introduces an error of less than ±2% in the absorption measurement. From these data a plot of the absorption cross section has been obtained which is shown in the lower part of Fig. 3. Our data are in good agreement with the absorption measurement for $HgI_2$ recently published by Maya.[18]

Since only a small fraction of the laser light is absorbed in the fluorescence cell over the wavelength region under investigation, and since the excited $I^*$ atom signal strength, $S(\lambda)$, varies linearly with the laser power, $S(\lambda)$ can be expressed as follows:

$$S(\lambda) = F \cdot N(\lambda) \cdot \phi(\lambda) \cdot \sigma(\lambda) \cdot n_c \qquad (1)$$

where $N(\lambda)$ is the number of photons at wavelength $\lambda$, $\phi(\lambda)$ is the quantum yield for $I^*$ atom production at wavelength $\lambda$, $\sigma(\lambda)$ is the absorption cross section at wavelength $\lambda$, $n_c$ is the number density of $HgI_2$ molecules, and F is a proportionality constant including transmission and collection efficiencies. A total of 19 measurements of the $I^*$ atom decay signal amplitude as a function of time were made at laser wavelengths ranging from 265 to 320 nm. The signal strength $S(\lambda)$ at each wavelength was obtained by an extrapolation of the observed exponential decay to time equal zero. The extrapolation of each signal curve is based on 8 data points over the decay signal using a least-squares fit method. Because of the finite signal-to-noise ratio of the measured signals, the intercept

at t = 0 can only be obtained with an accuracy of ±10%. The laser power was recorded continuously as described earlier, and from these measurements the number of photons at a specific wavelength, $N(\lambda)$, is determined by the relation $N(\lambda) = P_M \cdot \lambda / h \cdot c$, where $P_M$ is the measured value of the integrated total laser energy, h is Planck's constant and c the velocity of light. For each signal measurement 3200 laser pulses were used. The laser was operated at a repetition rate of 20 Hz, which amounts to a measurement time of 160 sec. During this time the output of the thermopile was recorded on an X-T recorder and $P_M$ has been obtained from an integration of the plotted power versus time curve using a planimeter. The accuracy of this method for obtaining the total laser energy for the 3200 pulses is estimated to be ±2%.

Since all quantities in Eq. (1), except F, are known from the measurements described above, the relative quantum yield for $I^*$ atom production $\phi(\lambda)$ can be determined. F describes the specific excitation and detection geometry, the absolute responsivity of the infrared detector, the transmission properties of the narrow band filter used, etc. It was obvious that the absolute value of this number could only be obtained by further elaborate measurements, each of which introduces additional errors. For this reason we chose a comparison method to determine the absolute value of $\phi(\lambda)$ for $HgI_2$. Branching ratios for the formation of excited $I^*$ and ground state I atoms upon broad band photolysis of a number of alkyl iodides have been obtained by Donohue and Wiesenfeld.[10,11] From this work it is known that the fractional yield for formation of $I^*$ atoms from n - $C_3F_7I$, for example, is greater than 0.99. Recent $I^*$ quantum yield measurements on n - $C_3F_7I$ as a function of wavelength from 280 to 320 nm show that the $I^*$ quantum yield is independent of the wavelength in this

region.[22] This compound has been used extensively in our laboratory to produce I* atoms for deactivation studies.[23] A simple additional measurement was performed to provide data on the ratio of I* production upon photodissociation of both $HgI_2$ and n - $C_3F_7I$. A modified fluorescence cell with a second sidearm, equipped with a stopcock, was used to allow the introduction of the n-perfluoropropyl-iodide from a storage bulb. Both stopcock and sidearm could be heated to prevent condensation of $HgI_2$ vapor in these parts of the cell. In the first run the cell and the $HgI_2$ containing sidearm were heated again to 453 K and 361 K respectively, while the second sidearm and the stopcock were kept at 423 K. The I* signal amplitude as well as the power of the laser light ($\lambda = 270$ nm) were recorded as described above. In the second run after condensation of $HgI_2$ into its sidearm, 0.3 Torr n-$C_3F_7I$ was introduced in the cell and the I* signal was measured in the identical manner at the same wavelength, $\lambda = 270$ nm. No change was made in the excitation and detection geometry and the same number of laser pulses (3200) was used.

The absorption cross section for $C_3F_7I$ was obtained from an absorption spectrum taken again with the commercial spectrometer, using a 5 cm path-length cell and 7 Torr of vacuum distilled n-$C_3F_7I$. In the upper part of Fig. 3 the results of this measurement are shown. Since, the signal amplitude, $S_{HgI_2} = F \cdot \phi_{HgI_2} \cdot \sigma_{HgI_2} \cdot n_{HgI_2}$ and $S_{C_3F_7I} = F \cdot \phi_{C_3F_7I} \cdot \sigma_{C_3F_7I} \cdot n_{C_3F_7I}$, where the symbols have been previously defined, we can now extract from the experimental data the ratio $\phi_{HgI_2}/\phi_{C_3F_7I}$ at $\lambda = 270$ nm without requiring a knowledge of the proportionality constant F. We find $\phi_{HgI_2}/\phi_{C_3F_7I} = 1.0 \pm 0.12$ where the quoted error is affected most by the extrapolation procedure to obtain the maximum amplitude of the fluorescence at time zero and by the temperature fluctuations in the fluorescence and

absorption cell. Using $\phi_{C_3F_7I} = 0.99$,[11] we obtain $\phi_{HgI_2} \cong 1$ at $\lambda = 270$ nm, within the error of the experiment. This calibration by comparison to n-$C_3F_7I$ at one specific wavelength provides an absolute calibration of the I* quantum yield as a function of wavelength upon photodissociation of $HgI_2$ over the entire wavelength region.

In Fig. 4 the final results of this photodissociation study of $HgI_2$ are shown. Curve A shows the region of the $HgI_2$ total absorption cross section which has been investigated. Curve B, which connects the measured points, is a plot of the product $\phi(\lambda) \cdot \sigma(\lambda)$ which is the fraction of the total absorption cross section associated with the excited I* atom production upon photodissociation. The quantum yield for I* formation $\phi(\lambda)$ can thus be obtained from the ratio "B/A" at each wavelength. The difference A-B has been plotted as well. The wavelength region where no measurements have been performed due to the lack of strong enough laser dyes is indicated. In this region a tentative interpolation is shown by the dashed line. A typical error bar of the measured points is given in the lower left part of the figure. The measured points have been corrected for the weakly wavelength dependent transmission of the quartz fluorescence cell windows. A decrease in transmission of 6% has been measured from 320 to 265 nm. The data have also been corrected for the small but finite wavelength dependent absorption of the laser light in the fluorescence cell. To complete the presentation of the measurements it should be mentioned that an I*-signal upon photodissociation of $HgI_2$ has also been observed at $\lambda = 248$ nm using a KrF excimer laser. Since the experimental apparatus had to be moved to perform this measurement, we were unable to properly scale this data point along with the rest. We can state, however, that the shorter wavelength region of the first absorption continuum of $HgI_2$ is also at least partly associated with states that lead to excited I* atom production.

## DISCUSSION

The essentially gas kinetic rate constant measured for the collisional deactivation of excited $I(5^2P_{1/2})$ atoms by the parent molecule $HgI_2$ ($k = 4.5 \times 10^{-10}$ cm$^3$ molecule$^{-1}$ sec$^{-1}$) suggests that a reactive exchange mechanism of the type $HgI_2 + I'^* \rightarrow HgI_2' + I$ ($\Delta H = -21.7$ kcal/mole) may be primarily responsible for the fast deactivation. Such types of mechanisms have been used to explain the fast deactivation observed in collisions of excited $I^*$ atoms and iodine molecules,[23] since the rate constants obtained for excited I atom deactivation by nonreactive molecules are typically one or two orders of magnitude smaller.[24,25] Since the heavy molecule $HgI_2$ is expected to be readily polarized by an approaching iodine atom, then attractive long range forces may lead to the formation of long-lived collision complexes with a subsequent decay into the relaxed reaction products. A second type of deactivating reaction collision which may be considered is $HgI_2 + I^* \rightarrow HgI + I_2$. However, this reaction is endothermic by 2.7 kcal/mole and is expected to be of minor importance. Additional deactivation mechanisms such as electronic-to-vibrational (E-V) energy transfer can, of course, not be excluded from contributing to the total rate.

The results obtained from the measurements of the $I^*$ quantum yield as a function of wavelength upon photodissociation (Fig. 4) suggest a relatively simple photodissociation mechanism in the first absorption continuum of $HgI_2$. The total absorption cross section is composed of two distinct components. The first component, with a maximum at 270 nm, is associated with the formation of excited $I^*(5^2P_{1/2})$ atoms, while the second component (difference A-B in Fig. 4), with a maximum around 310 nm, most likely now can be attributed to the formation of ground state $I(5^2P_{3/2})$ atoms. Numerous electronically excited states of $HgI_2$ may participate in the absorption

in the region of 265 to 320 nm, however the observed behavior may be simply described by just two such states. Since no bound excited states of $HgI_2$ are known below 6 eV from previous spectroscopic studies, we assume that only purely repulsive electronically excited states are being accessed in the first absorption continuum. In Fig. 5 two highly simplified schemes of potential curves are shown, which can explain qualitatively the formation of both excited and ground state iodine atoms upon photodissociation of $HgI_2$. The diagrams (a) and (b) show, only schematically, the potential energy of the linear, symmetric $HgI_2$ molecule as a function of the IHg - I distance. Known spectroscopic details, such as the energy of the IHg - I bond (2.6 eV) and the energy of the excited $I(5^2P_{1/2})$ state (0.94 eV) have been used in constructing the figure. The $HgI_2$ molecule has been shown to be linear, with an equilibrium Hg-I bond distance of 2.61 Å.[26] The approximate shape and locations of the schematic potential surfaces can be obtained from these details, along with the component spectral features shown in Fig. 4. From the multitude of excited states of $HgI_2$ which will be formed by interacting the ground state of the HgI ($X^2\Sigma$) molecule with a ground ($^2P_{3/2}$) and excited ($^2P_{1/2}$) iodine atomic states, only two are tentatively indicated in each diagram to serve as model potential curves in the explanation of the observed results. In Fig. 5(a) two non-crossing repulsive excited states are shown correlating to a ground state HgI ($X^2\Sigma$) molecule and excited I* and ground state I atoms respectively. On the basis of this model one would expect, from simple Franck-Condon arguments and assuming symmetry allowed transitions from the ground state, two absorption maxima. According to the observed photofragment spectrum, the first absorption around 270 nm correlates with excited $I(5^2P_{1/2})$ atoms at infinite internuclear distance while the absorption around 310 nm leads to ground state $I(5^2P_{3/2})$ atoms. A second

possible model for the potential curves of $HgI_2$ is shown in Fig. 5(b). In this case the two repulsive states undergo a curve crossing at an internuclear distance greater than the equilibrium distance $[R(IHg - I)]_{eq}$ of the $HgI_2$ molecule. Assuming the same molecular symmetry for both repulsive states an interaction at the crossing point allows transitions between the two states. In this model, the absorption of photons would reach only the excited state (1), and the branching ratio for formation of excited and ground state iodine atoms is determined by Landau-Zener type transition probabilities at the crossing point. A decreasing probability for transitions from state (1) to state (2) is expected for increasing relative velocities of the dissociating fragments, HgI + I. On the basis of this model one would predict predominantly greater excited $I^*$ atom yields at shorter wavelengths and predominant formation of ground state I atoms at longer wavelengths, where the relative velocity of the separating fragments is lower. Such a model would explain the observed results well, since at 320 nm almost exclusively ground state I atoms are produced upon photodissociation of $HgI_2$ and at 270 nm, $I^*$ is the major photofragment product. It is not possible to experimentally distinguish between these two different schemes for the potential curves. Of course, more information can be obtained from a measurement of the relative kinetic energy of the departing fragments, as well as a determination of the internal energy of the HgI fragment after the photodissociation. Such measurements will be necessary to obtain a more complete picture of the shape and the nature of the mutual interaction of the electronically excited states participating in the photodissociation of $HgI_2$.

From the quantum yield results presented above, it is evident that

the $HgI_2$ molecule might make an interesting new source for the 1.315 μm $I^*$ laser. In most of the high power $I^*$ lasers designed for laser fusion applications, photolytically pumped $C_3F_7I$ and other alkyl iodides are used as the active medium.[27] One disadvantage of this laser is that the alkyl iodides have to be recycled continuously in a closed fast flow circulating system to purify and regenerate the parent compound from photolysis products. Our results and the results of Schimitschek[12] indicate that $HgI_2$ is chemically reversible upon photodissociation. After tens of thousands of laser pulses at repetition rates of 20 Hz and pulse energies of the order of 1 mJ, no deviations in the amplitude and time behavior of the $I^*$ signals are observed other than the normal statistical fluctuations. There would be several advantages and disadvantages in using $HgI_2$ as a source for an $I^*$ laser. As can be seen from Fig. 3 the absolute value of the absorption cross section for $HgI_2$ at 270 nm is more than 20 times larger than for n - $C_3F_7I$. This would allow for efficient production of a comparable number of $I^*$ atoms upon photodissociation of $HgI_2$ at accordingly lower pressures. The $I^*$-quantum yield upon photodissociation of $HgI_2$ is essentially unity at 270 nm. This number decreases towards longer wavelengths, however, most of the first absorption continuum leads to excited $I^*$ atom production. It has not been determined at this time whether the other regions of the $HgI_2$ absorption bands are also associated with efficient $I^*$ production upon photodissociation. With further investigation, the $HgI_2$ system might make an interesting $I^*$ source by broadband photolysis. The very rapid quenching of $I^*$ by $HgI_2$ is a serious drawback, and would make it necessary to pump the $HgI_2$ at a faster rate and at lower pressures than $C_3F_7I$ in order to maintain the same level of population inversion. A proper

matching of the time duration of the pumping light pulse and $HgI_2$ pressure appears feasible but technologically more difficult. Because of the large absorption cross section of $HgI_2$ it might be possible to completely photobleach the sample with optical pumping. The deactivation rate of $I^*$ will then be determined by the quenching with the HgI and $I^*$ fragments produced and not the parent $HgI_2$. Slower rate constants associated with collisional deactivation by those fragments would correspondingly enhance the feasibility of conventional optical pumping. Minor technological advances must be made to operate such a device at the mild temperatures (~500 K) needed to generate the $HgI_2$ vapor. Finally the possibility of using an electric discharge based pumping scheme where excitation pulses can be generated which are orders of magnitude shorter than those of conventional flashlamps should not be overlooked. $HgBr_2$, for example, has been dissociated by electron collisions in a transverse electric discharge and lasing action observed on the $B^2\Sigma \rightarrow X^2\Sigma^+$ transition of HgBr.[14] With appropriate electron energies it should be possible to produce $I^*$ by electron excitation into the first long wavelength absorption band as well. Fast discharge excitation would eliminate the problems associated with the rapid collisional deactivation of excited iodine atoms by $HgI_2$.

## Acknowledgments

We want to thank S. L. Baughcum for help with the experiment involving the excimer laser. The authors gratefully acknowledge the support of the Office of Naval Research and the National Science Foundation.

References

*Staff member, Quantum Physics Division, National Bureau of Standards; and Alfred P. Sloan Fellow.

1. J. P. Simons, in Gas Kinetics and Energy Transfer, edited by P. G. Ashmore and R. J. Donovan (The Chemical Society, London, 1977), Vol. 2.
2. G. E. Busch, J. R. Cornelius, R. T. Mahoney, R. I. Morse, D. W. Schlosser and K. R. Wilson, Rev. Sci. Instr. 41, 1066 (1970).
3. K. R. Wilson, in Excited State Chemistry, edited by J. N. Pitts, Jr. (Gordon and Breach, New York, 1970).
4. G. A. Hancock and K. R. Wilson, in Fundamental and Applied Laser Physics, Proceedings of the Esfahan Symposium, edited by M. Feld, A. Javan and N. Kurmit (Wiley, New York, 1973).
5. J. A. Coxon, in Molecular Spectroscopy, edited by R. F. Barrow, D. A. Long and D. J. Millen (The Chemical Society, London, 1973), Vol. 1.
6. R. N. Zare and D. R. Hershbach, Atomic and Molecular Fluorescence Excited by Photodissociation, Appl. Opt. Suppl. No. 2 (1965).
7. J. V. V. Kasper and G. C. Pimentel, Appl. Phys. Lett. 5, 231 (1964).
8. S. J. Riley and K. R. Wilson, Discuss. Faraday Soc. 53, 132 (1972).
9. M. Dzvonik, S. Yang and R. Bersohn, J. Chem. Phys. 61, 4408 (1974).
10. T. Donohue and J. R. Wiesenfeld, Chem. Phys. Lett. 33, 176 (1975).
11. T. Donohue and J. R. Wiesenfeld, J. Chem. Phys. 63, 3130 (1975).
12. S. J. Davis, Appl. Phys. Lett. 32, 656 (1978).
13. E. J. Schimitschek, J. E. Celto and J. A. Trias, Appl. Phys. Lett. 31, 608 (1977).
14. E. J. Schimitschek and J. E. Celto, Opt. Lett. 2, 64 (1978).
15. A. Terenin, Z. Phys. 44, 713 (1927).

16. K. Wieland, Z. Phys. 76, 801 (1932).

17. K. Wieland, Z. Elektrochem. 64, 761 (1960).

18. J. Maya, J. Chem. Phys. 67, 4976 (1977).

19. Handbook of Chemistry and Physics, 52nd Ed., 1971-1972.

20. D. R. Stull and H. Prophet, Natl. Stand. Ref. Data Ser. 37 (1971).

21. R. H. Garstang, J. Res. Nat. Bur. Stand. A68, 61 (1964).

22. F. J. Comes, private communication.

23. H. Hofmann and S. R. Leone, J. Chem. Phys., in press.

24. R. J. Donovan and D. Husain, Chem. Rev. 70, 489 (1970).

25. D. Husain and R. J. Donovan, Adv. Photochem. 8, 1 (1971).

26. P. W. Allen and L. E. Sutton, Acta Cryst. 3, 46 (1950).

27. K. Hola, G. Brederlow, E. Fill, R. Volk and K. J. Witte, Prospects of the High Power Iodine Laser, IPP Report IV/93 (Max Planck-Institut für Plasmaphysik, München).

Figure Captions

Fig. 1. Experimental apparatus for tunable laser photofragmentation studies.

Fig. 2. Rate versus pressure results of the collisional deactivation of $I(5^2P_{1/2})$ atoms by the parent molecule $HgI_2$.

Fig. 3. Absolute absorption cross sections for $n$-$C_3F_7I$ (upper part) and $HgI_2$ (lower part), derived from measured absorption spectra in this work. The investigated wavelength range in the photodissociation study of $HgI_2$ is indicated by the shaded area.

Fig. 4. Total absorption cross section of $HgI_2$ and fractional components leading to excited $I(5^2P_{1/2})$ and ground state $I(5^2P_{3/2})$ atoms upon photodissociation of $HgI_2$.

Fig. 5. Two possible potential curve schemes for $HgI_2$, serving as models in the interpretation of the experimental photofragment results.

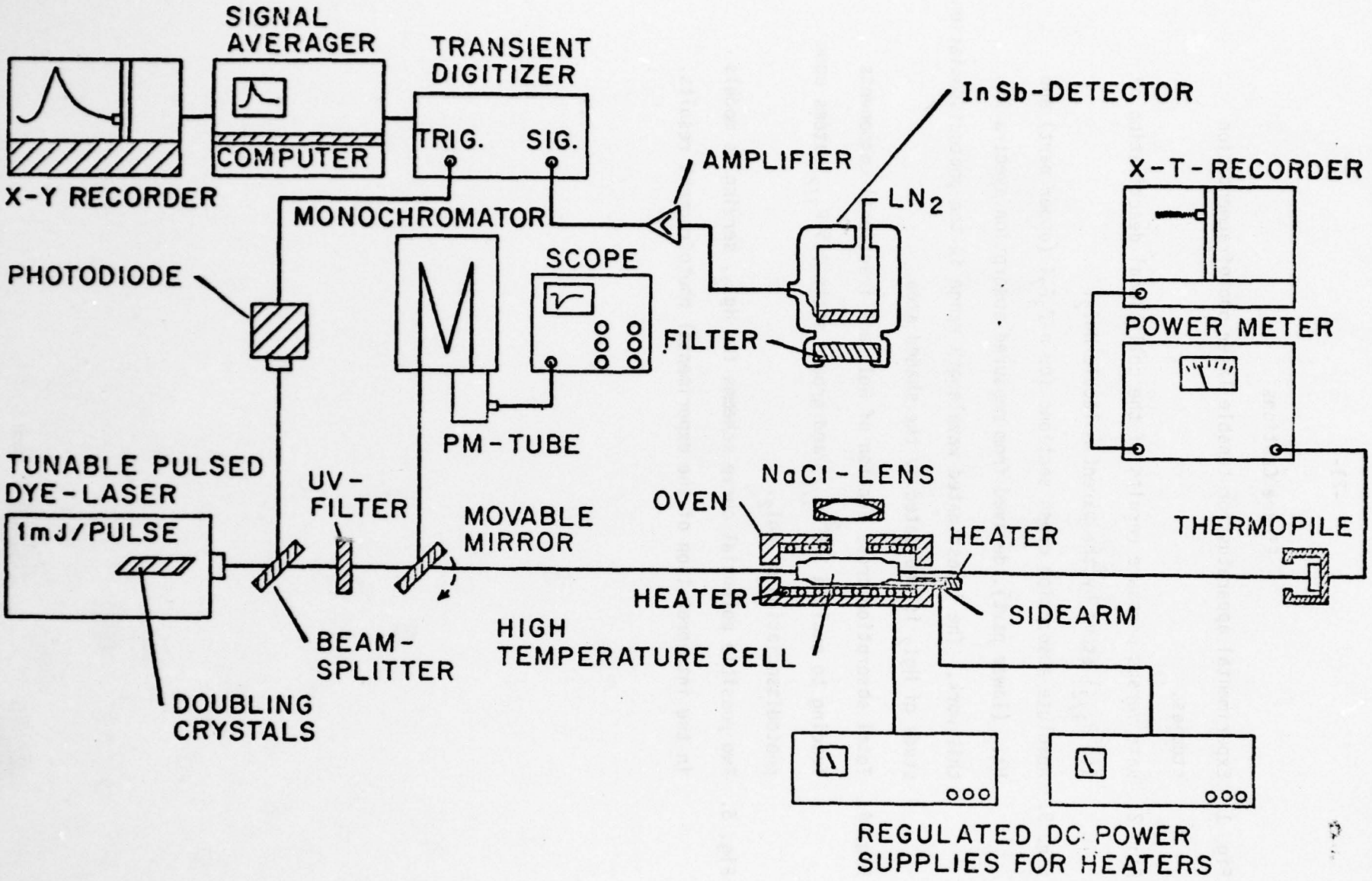
SIGNAL AVERAGER
TRANSIENT DIGITIZER
InSb-DETECTOR
TRIG.
SIG.
COMPUTER
X-Y RECORDER
AMPLIFIER
X-T-RECORDER
LN2
MONOCHROMATOR
PHOTODIODE
SCOPE
FILTER
POWER METER
PM-TUBE
TUNABLE PULSED DYE-LASER
UV-FILTER
NaCl-LENS
OVEN
MOVABLE MIRROR
HEATER
THERMOPILE
1mJ/PULSE
HEATER
SIDEARM
BEAM-SPLITTER
HIGH TEMPERATURE CELL
DOUBLING CRYSTALS
REGULATED DC POWER SUPPLIES FOR HEATERS

Figure 1

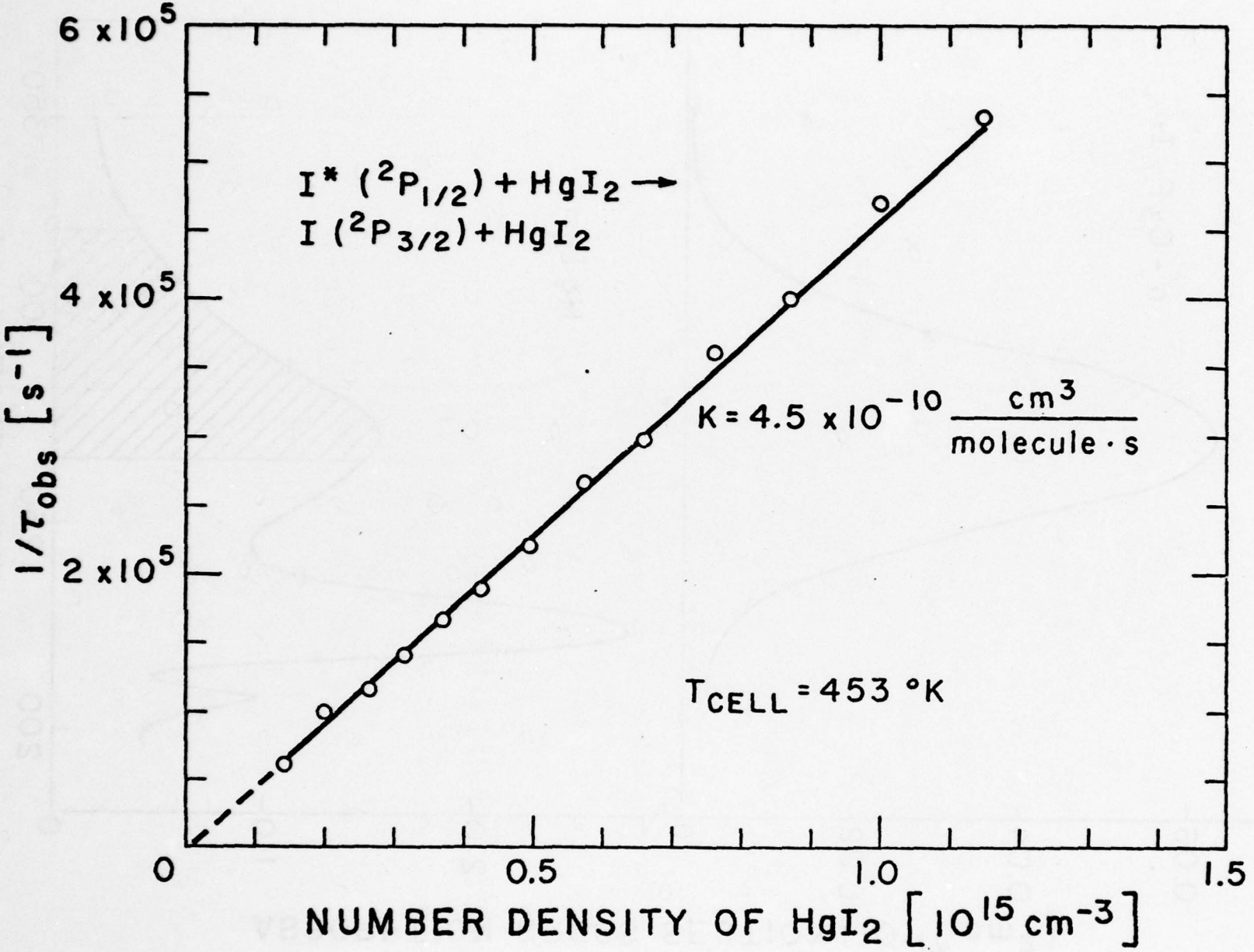
6 x10^5
4 x10^5
2 x10^5
0
0.5
1.0
1.5
1/τobs [s^-1]
I* (2P1/2) + HgI2 →
I (2P3/2) + HgI2
K = 4.5 x10^-10 cm^3 / molecule · s
TCELL = 453 °K
NUMBER DENSITY OF HgI2 [10^15 cm^-3]

Figure 2

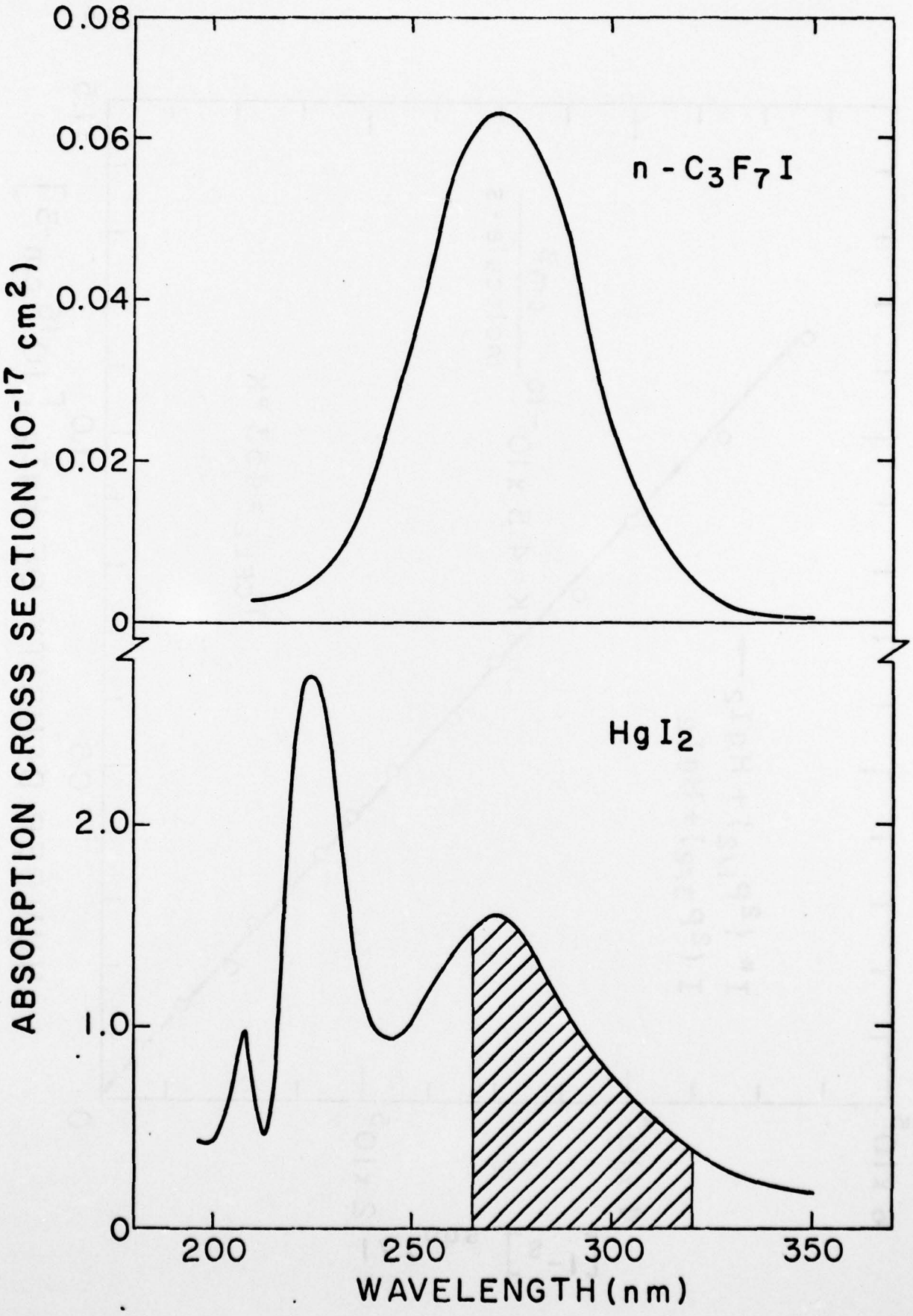
0.08
0.06
0.04
0.02
0
n - C3F7I
HgI2
2.0
1.0
0
200
250
300
350
WAVELENGTH (nm)
ABSORPTION CROSS SECTION (10-17 cm2)

Figure 3

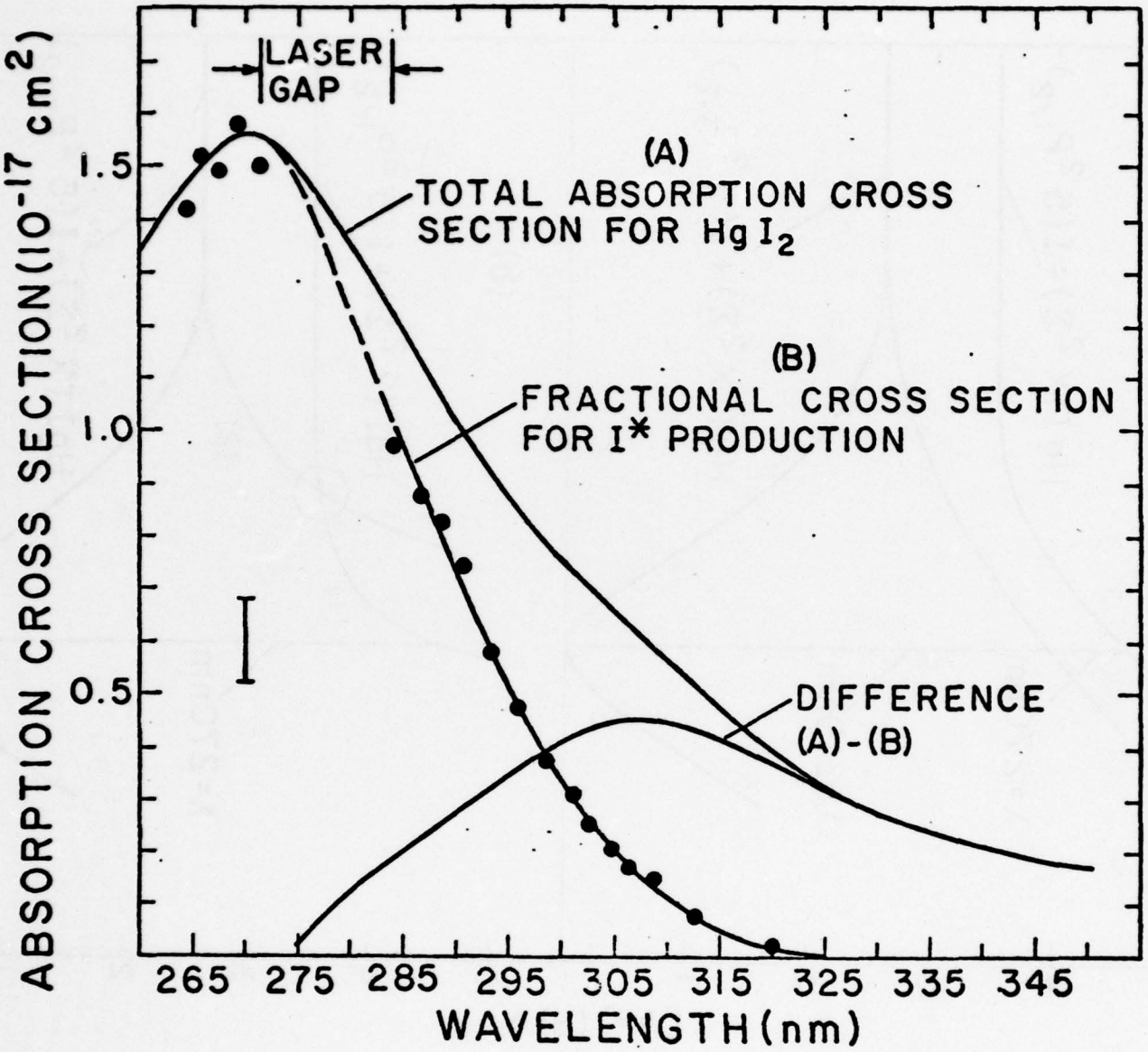
LASER
GAP
(A)
TOTAL ABSORPTION CROSS
SECTION FOR $HgI_2$
(B)
FRACTIONAL CROSS SECTION
FOR I* PRODUCTION
DIFFERENCE
(A)-(B)
ABSORPTION CROSS SECTION ($10^{-17}$ $cm^2$)
1.5
1.0
0.5
265 275 285 295 305 315 325 335 345
WAVELENGTH (nm)

Figure 4

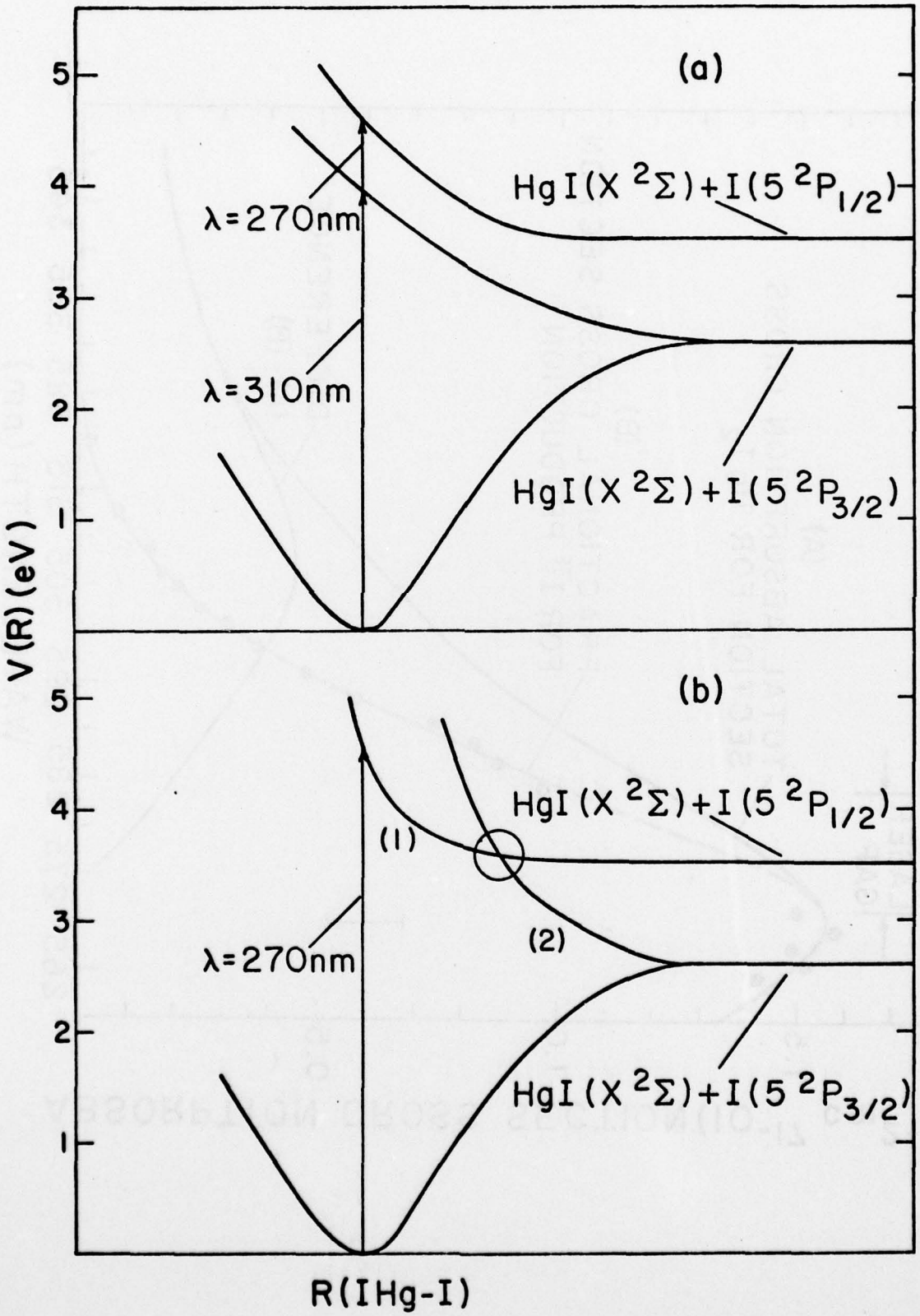
(a)
HgI(X $^2\Sigma$)+I(5 $^2P_{1/2}$)
λ=270nm
λ=310nm
HgI(X $^2\Sigma$)+I(5 $^2P_{3/2}$)
(b)
HgI(X $^2\Sigma$)+I(5 $^2P_{1/2}$)
(1)
(2)
λ=270nm
HgI(X $^2\Sigma$)+I(5 $^2P_{3/2}$)
V(R)(eV)
R(IHg-I)
1
2
3
4
5

Figure 5